# Epipolar Consistency Conditions for Motion Correction in Weight-Bearing Imaging

Bastian Bier[1], André Aichert[1], Lina Felsner[1], Mathias Unberath[1], Marc Levenston[2], Garry Gold[2], Rebecca Fahrig[2], Andreas Maier[1]

[1]Lehrstuhl für Mustererkennung, Friedrich-Alexander-Universität Erlangen-Nürnberg
[2]Department of Radiology, School of Medicine, Stanford University, USA
bastian.bier@fau.de

**Abstract.** Recent C-arm CT systems allow for the examination of a patient's knees under weight-bearing conditions. The standing patient tends to show involuntary motion, which introduces motion artifacts in the reconstruction. The state-of-the-art motion correction approach uses fiducial markers placed on the patients' skin to estimate rigid leg motion. Marker placement is tedious, time consuming and associated with patient discomfort. Further, motion on the skin surface does not reflect the internal bone motion. We propose a purely projection based motion estimation method using consistency conditions of X-ray projections. The epipolar consistency between all pairs of projections is optimized over various motion parameters. We validate our approach by simulating motion from a tracking system in forward projections of clinical data. We visually and numerically assess reconstruction image quality and show an improvement in Structural Similarity from 0.912 for the uncorrected case to 0.943 using the proposed method with a 3D translational motion model. Initial experiments showed promising results encouraging further investigation of practical applicability.

## 1 Introduction

Recent C-arm cone-beam CT systems support flexible trajectories, including horizontal scans of the knee joint in standing position under weight-bearing conditions [1]. These trajectories allow for the observation of knee kinematics under load [2], which might lead to a better understanding of knee cartilage health. A major problem of the acquisition is involuntary patient motion during the scan. Different motion correction methods have been proposed to mitigate motion artifacts in reconstructed images. The state-of-the art method uses fiducial markers and applies a 3D rigid motion to the estimated 3D marker positions, aligning them with detected 2D marker positions on the detector [3,4,5]. However, marker placement is tedious, since they have to be placed such that they do not overlap in the projection images. This leads to longer examination time and patient discomfort. In addition, skin motion may not optimally represent the actual joint motion. Another approach by Berger et al. [6] uses bone segmentations of a previously acquired supine acquisition and performs a 2D/3D registration of the segmented bone with the projection images. However, a previously acquired motion free reconstruction is rarely available and the method is computationally highly expensive. Other approaches are purely image [7] or projection-based [8]. Sisniega et al. evaluate a sharpness measure to estimate sub-millimeter motion, but are restricted to a small region of interest [7]. Unberath et al. use maximum intensity projections from an initial reconstruction to align the bone outlines in 2D [8].

In this work, we investigate another purely projection-based motion correction method using Epipolar Consistency Conditions (ECC) [9]. ECC can be used to define a consistency metric on the relative geometry of any pair of X-ray images, which can be optimized for motion parameters. We tried 3 motion models: 2D detector shifts, 3D patient translation, and a rigid 3D patient motion. Experiments on a clinical supine acquisition were performed, where real patient motion is used to simulate motion corrupted projection images.

# 2 Materials and Methods

## 2.1 Epipolar Consistency Conditions

Epipolar Consistency Conditions (ECC) are conditions on corresponding line integrals in two pre-processed X-ray projections $I_0$, $I_1$. Their respective source positions define a pencil of planes $\mathbf{E}^\kappa$ around the baseline, associated with an angle $\kappa$ to the iso-center. By intersection with the detectors, any such plane defines two lines $\mathbf{l}_0^\kappa$, $\mathbf{l}_1^\kappa \in \mathbb{P}^2$ in oriented projective space of the images, which both contain information of the same plane $\mathbf{E}^\kappa$ through the object. ECC allow us to express a metric of inconsistency using integrals of such lines

$$\frac{\partial}{\partial t}\rho_{I_0}\left(\mathbf{l}_0^\kappa\right) - \frac{\partial}{\partial t}\rho_{I_1}\left(\mathbf{l}_1^\kappa\right) \approx 0,$$

where $\rho_I(\mathbf{l})$ denotes the integral over line $\mathbf{l} = (-\sin(\alpha), \cos(\alpha), -t)^\top \in \mathbb{P}^2$ of angle $\alpha$ and distance to the image origin $t$, in projective space of image $I$ . The inconsistency metric for two projection indices $i$ and $j$ is

$$ECC_i^j = \int\limits_{[-\frac{\pi}{2},\frac{\pi}{2}]} \left(\frac{\partial}{\partial t}\rho_{I_j}\left(\mathbf{l}_j^\kappa\right) - \frac{\partial}{\partial t}\rho_{I_i}\left(\mathbf{l}_i^\kappa\right)\right)^2 d\kappa$$

## 2.2 Motion Model

Given the geometry of the $j$-th image, defined by a projection matrix $\mathbf{P}_j \in \mathbb{R}^{3\times4}$, $j \in \{1, \ldots, n\}$, we can model detector shifts and rigid patient motion simply by matrix-multiplication $\mathbf{P}'_j = \mathbf{H}_j \cdot \mathbf{P}'_j \cdot \mathbf{T}_j$, with

$$\mathbf{H}_j = \begin{pmatrix} 1 & 0 & d_u^j \\ 0 & 1 & d_v^j \\ 0 & 0 & 1 \end{pmatrix} \text{ and } \mathbf{T}_j = \begin{pmatrix} \mathbf{R}_j & \mathbf{t}_j \\ \mathbf{0} & 1 \end{pmatrix},$$

where $d_u^j$ and $d_v^j$ denote detector domain shifts and $\mathbf{T}_j$ is a rigid patient motion in 3D comprised of a translation vector $\mathbf{t}_j \in \mathbb{R}^3$ and a rotation about the iso-center $\mathbf{R}_j \in SO(3, \mathbb{R})$, defined by Euler-angles $\mathbf{r} = \left(r_x^j,\, r_y^j, r_z^j\right)^\top$.

### 2.3 Optimization

Let $M(\boldsymbol{\phi})$ denote the sum over $ECC_i^j$ for all ordered pairs of projections $\{i,\, j\} \subset \{1, \ldots, n\}^2$, transformed according to Section 2.2, where the parameter vector $\boldsymbol{\phi}$ may contain only detector shifts $\boldsymbol{\phi}^{2D} = \left(d_u^1,\, d_v^1 \ldots d_u^n,\, d_v^n\right)^\top$, translation vectors $\boldsymbol{\phi}^{3D} = (\mathbf{t}_1, \ldots, \mathbf{t}_n)^\top$, or full 6D rigid transformations $\boldsymbol{\phi}^{6D} = (\mathbf{t}_1,\, \mathbf{r}_1 \ldots, \mathbf{t}_n\, \mathbf{r}_n)^\top$. We then minimize the inconsistencies

$$\boldsymbol{\phi}^\star = \underset{\boldsymbol{\phi}}{\operatorname{argmin}}\, M(\boldsymbol{\phi}),$$

using gradient-free numerical optimization. To reduce the total number of parameters, we run $n$ successive optimizations of parameters for only one projection, and repeat this procedure until the solution has sufficiently converged.

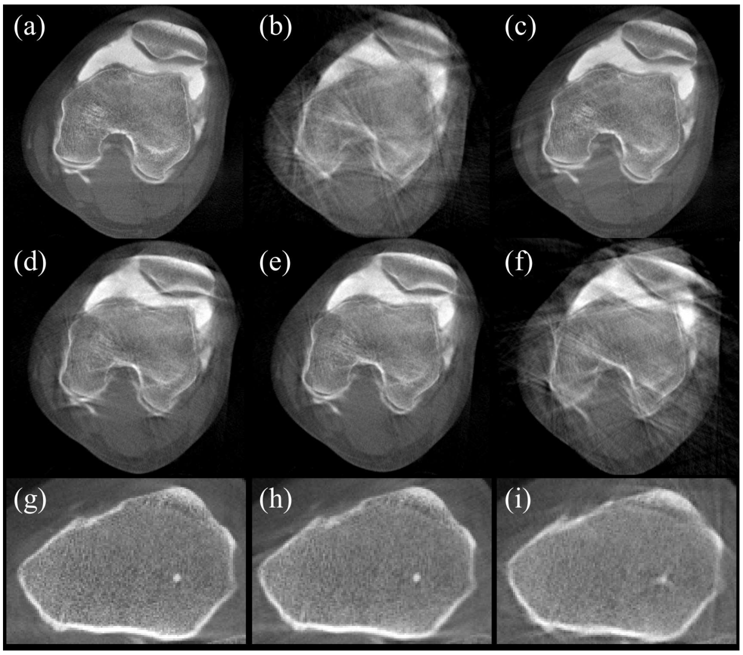


**Fig. 1.** Reconstructed images. Ground truth (a), No correction (b), Müller et al. [5] Marker Based (c), Proposed method optimized 2D shifts (d), 3D translation (e) and 6D rigid motion (f). The last row (g)-(i) shows detail views of (a), (c) and (e) at a different slice.

### 2.4 Experiments

All experiments use the geometry of a real acquisition with 248 projections with a detector size of 1240×960. Reconstruction was performed using a standard FDK with a sharp kernel. We forward projected a high quality supine reconstruction of the knees under 3D rigid motion. The motion parameters are taken from a real patient measured with a motion capture system, while performing a squat with $60^\circ$ flexion [3]. We compared the reconstructions using our novel approach (estimating either 2D detector shifts, 3D translation or 6D rigid motion) with the ground truth motion free reconstruction, the motion corrupted reconstruction, and the state-of-the-art marker-based approach [5]. We calculated the Structural Similarity (SSIM) and further analyzed the estimated parameters.

## 3 Results

Figure 1 shows motion-compensated 3D reconstructions. Without any motion correction, streaks and blurring artifacts are present, compare Figure 1b. ECC motion estimation with 2D detector shifts and 3D translation (Fig. 1d and Fig. 1e) considerably improved image quality, while results for 3D rigid motion were not as good (Fig. 1f). Using the state-of-the-art marker-based approach, only some motion induced streak artifacts remain, see Figure 1c. A detail view in Figure 1(g)-(i) shows that image quality for the state-of-the-art method is still slightly better.

Further, we registered all reconstructions to the ground truth result and computed the SSIM, shown in Table 1. Our method peaks at a SSIM of 0.943 and shows an improvement compared to the uncorrected case with an SSIM of 0.912. The best result is achieved by state-of-the-art with a SSIM of 0.987.

In the following, we only show the results of our best results, which has been the estimation of 3D tranlation. Figure 2 shows a comparison to ground truth motion parameters. Note, that the ground truth and the state-of-the-art method are based on a rigid model with additional rotation, whereas our method only estimates translations. Generally, the motion is recovered well for both methods. Noticeable is the peak of the state-of-the-art method around projection 45. In these views, markers overlap in the projection images and thus motion estimation becomes inaccurate, which leads to the streaks in the reconstruction. Further, the proposed method reproduces high frequencies of the motion signal in the middle views and the beginning and the end of the Y-parameter very accurately, while the Z-parameter is generally roughly recovered.

We now focus on the X-parameter in the top row in Figure 3. Observe, that an accurate estimation of the high frequencies is possible in areas, where the object motion is parallel to the detector. In other words, our method estimates motion along the viewing direction less accurately. Note however, that such motion can be observed in the images only as a small scaling and thus has less effect on the reconstruction than motion parallel to the detector. This fact is visualized in the bottom row in Figure 3, where the translation vector is projected onto the detector plane.

## 4 Discussion

We suggest a novel projection-based method to estimate patient motion during knee-scans under weight-bearing conditions. Our method exploits redundancies in projection domain to optimize the consistency over patient motion parameters, and unlike state-of-the-art methods requires neither a reference scan in supine position nor fiducial markers attached to the patient. We validate the approach on forward projections of real patient data under real patient motion.

In our experiments we compensate for 3D patient motion using 2D detector shifts, 3D translations and full 6D rigid motion. For 2D and 3D models, we are able to show considerable improvements when compared to no compensation, although state-of-the-art marker-based compensation yields slightly better results. This is expected, since we do not model rotations.

For practical applicability, future work must address several current limitations. First, we currently assume that only one leg is visible in the projection images. However, with our clinical setup it is not realistic to have a patient stand on one leg and it is not feasible to separate the legs in the projection domain. Second, the field-of-view of a C-arm is too small to always fit both legs, resulting in major truncation. Truncation may be problematic as an additional source of inconsistency. Third, epipolar consistency has been shown to be capable of correcting 6DOF rigid motion in other applications [10].

Despite current limitations, this paper presents the first step towards using consistency conditions for extremity imaging, mitigating the need for markers or an additional supine scan. In addition to being computationally feasible, the motion is estimated directly on the bones, instead of on the skin surface.

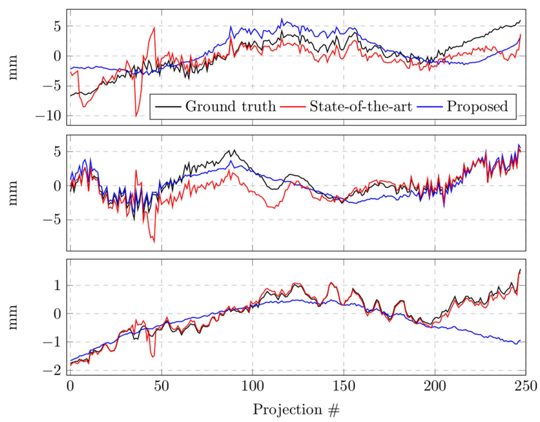


**Fig. 2.** Raw motion parameters x, y and z.

**Tab. 1. Structural similarity (SSIM) results.**

| Method | SSIM |
|---|---|
| Uncorrected | 0.912 |
| State-of-the-art [5] | 0.987 |
| 2D shifts | 0.933 |
| 3D translation | 0.943 |
| 6D rigid motion | 0.892 |

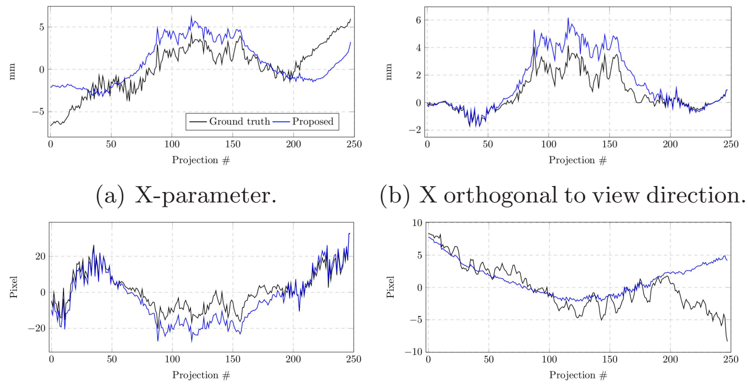


(a) X-parameter.

(b) X orthogonal to view direction.

(c) u-component of the projected translation on detector.

(d) v-component of the projected translation on the detector.

**Fig. 3.** Analysis of the translation vector in view direction and detector projection.

## References

1. Maier A, Choi JH, Keil A, Niebler C, Sarmiento M, Fieselmann A, et al. Analysis of vertical and horizontal circular C-arm trajectories. Proc SPIE. 2011;7961:796123–1–796123–8.
2. Powers CM, Ward SR, Fredericson M. Knee Extension in Persons With Lateral Subluxation of the Patella : A Preliminary Study. J Orthop Sports Phys Ther. 2013;33(11):677–685.
3. Choi JH, Fahrig R, Keil A, Besier TF, Pal S, McWalter EJ, et al. Fiducial marker-based correction for involuntary motion in weight-bearing C-arm CT scanning of knees. Part I. Numerical model-based optimization. Med Phys. 2014;41(6):061902.
4. Choi JH, Maier A, Keil A, Pal S, McWalter EJ, Beaupré GS, et al. Fiducial marker-based correction for involuntary motion in weight-bearing C-arm CT scanning of knees. II. Experiment. Med Phys. 2014;41(6):061902.
5. Müller K, Berger M, Choi J, Maier A, Fahrig R. Automatic Motion Estimation and Compensation Framework for Weight-bearing C-arm CT scans using Fiducial Markers. Proc IFMBE. 2015; p. 58–61.
6. Berger M, Müller K, Aichert A, Unberath M, Thies J, Choi JH, et al. Marker-free motion correction in weight-bearing cone-beam CT of the knee joint. Med Phys. 2016;43(3):1235–1248.
7. Sisniega A, Stayman JW, Cao Q, Yorkston J, Siewerdsen JH, Zbijewski W. Image-based motion compensation for high-resolution extremities cone-beam CT. Proc SPIE. 2016;9783:97830K.
8. Unberath M, Choi JH, Berger M, Maier A, Fahrig R. Image-based compensation for involuntary motion in weight-bearing C-arm cone-beam CT scanning of knees. Proc SPIE. 2015;9413:94130D.
9. Aichert A, Breininger K, Köhler T, Maier A. Efficient epipolar consistency. Proc CT Meeting 2016. 2016; p. 259–262.
10. Aichert A, Wang J, Schaffert R, Dörfler A, Hornegger J, Maier A. Epipolar Consistency in Fluoroscopy for Image-Based Tracking. Proc BMVC. 2015; p. 82.1–82.10.